Middle East Research Journal of Engineering and Technology
ISSN: 2789-7737 (Print) ISSN: 2958-2059 (Online)
Frequency: Bi-Monthly
DOI: https://doi.org/10.36348/merjet.2025.v05i04.002

KUWAIT SCHOLARS PUBLISHER
Website: http://www.kspublisher.com/
Email: office@kspublisher.com

Strength and Chloride Resistance of Underground Buried Steel Pipe Coated with Albizia Ferruginea Exudates

Sarogoro Ndenebari Samuel[1], Oruene Watson Daibi[2], Charles Kennedy[1*]
[1]School of Engineering, Department of Civil Engineering, Kenule Beeson Saro-Wiwa Polytechnic, Bori, Rivers State, Nigeria
[2]School of Engineering, Department of Mechanical Engineering, Kenule Beeson Saro-Wiwa Polytechnic, Bori, Rivers State, Nigeria

Abstract: This study investigates the effectiveness of Albizia ferruginea exudates as a protective coating for underground buried steel pipelines, focusing on its corrosion resistance and mechanical properties. The results indicate that the application of these natural coatings significantly enhances the structural integrity of steel while providing effective corrosion protection. Coated samples showed a corrosion potential (Ecorr) ranging from -600 mV to -500 mV versus the saturated calomel electrode (SCE), in contrast to uncoated samples, which displayed values between -450 mV and -400 mV. Furthermore, the corrosion current density (Icorr) for coated samples ranged from 0.01 to 0.05 µA/cm², while uncoated samples exhibited values between 0.1 and 0.5 µA/cm². Mechanical properties also improved significantly: tensile strength for coated samples was between 450 and 500 MPa compared to 350 to 400 MPa for uncoated samples, and yield strength ranged from 250 to 300 MPa for coated samples versus 200 to 225 MPa for uncoated samples. These findings confirm that Albizia ferruginea exudates not only act as effective corrosion inhibitors but also enhance the mechanical performance of steel under stress.

Keywords: Albizia Ferruginea, Corrosion Resistance, Mechanical Properties, Natural Coatings, Impedance.

Research Paper

***Corresponding Author:**
Charles Kennedy
School of Engineering, Department of Civil Engineering, Kenule Beeson Saro-Wiwa Polytechnic, Bori, Rivers State, Nigeria

How to cite this paper:
Sarogoro Ndenebari Samuel *et al* (2025). Strength and Chloride Resistance of Underground Buried Steel Pipe Coated with Albizia Ferruginea Exudates. *Middle East Res J. Eng. Technol, 5*(4): 63-78.

Article History:
| Submit: 13.06.2025 |
| Accepted: 10.07.2025 |
| Published: 14.07.2025 |

1. INTRODUCTION

The corrosion of steel pipes buried underground presents a formidable challenge across multiple industries, particularly in oil and gas transportation, water distribution systems, and sewage management infrastructure (Koch *et al*., 2016; Yahaya *et al*., 2011). This phenomenon carries substantial financial burdens and environmental hazards with cascading effects on public safety and economic stability (Papavinasam, 1999; NACE International, 2016). The annual global cost of corrosion-related damage exceeds $2.5 trillion, with buried pipelines accounting for approximately 30% of these losses (Koch *et al*., 2016; Adikari & Munasinghe, 2016). Corrosion systematically degrades pipeline structural integrity, leading to catastrophic failures such as leaks and ruptures requiring expensive remediation efforts (Parker & Peattie, 1984; Kiefner & Rosenfeld, 2012). These incidents disrupt critical infrastructure and pose severe environmental risks, including soil and groundwater contamination persisting for decades (Wiese, 2015; Usman *et al*., 2019).

Among factors contributing to underground pipe corrosion, chloride ions in soil and groundwater represent one of the most aggressive corrosive agents (Li *et al*., 2007; Krivy *et al*., 2017). These ions accelerate corrosion by penetrating protective oxide layers, disrupting passivation films, and creating localized electrochemical cells promoting pitting corrosion (Verma *et al*., 2018; Arriba-Rodriguez *et al*., 2018). The situation becomes particularly severe in coastal regions with saltwater intrusion and industrial areas using de-icing salts (Chaker, 1989; Pereira *et al*., 2015). Research indicates chloride-induced corrosion rates can increase by up to 400% when soil moisture rises from 10% to 30%, demonstrating synergistic effects (Yahaya *et al*., 2011; Dang *et al*., 2015).

Advances in corrosion protection focus on multi-layered defense strategies combining physical barriers with electrochemical protection (Chen & Zhao, 2017; Brycki *et al*., 2018). Natural coatings derived from plant exudates have emerged as particularly promising due to environmental sustainability and cost-effectiveness (Marzorati *et al*., 2018; Chigondo & Chigondo, 2016). Albizia ferruginea exudates demonstrate exceptional corrosion inhibition properties owing to their unique biochemical composition (Fouda *et al*., 2017; Okewale & Olaitan, 2017). These natural resins contain high concentrations of polyphenolic

compounds, including tannins and flavonoids, forming stable chelate complexes with iron ions on steel surfaces (Banerjee *et al*., 2012; Ameh & Eddy, 2016). Their molecular structure enables strong adsorption onto metal substrates, creating hydrophobic barriers significantly reducing oxygen diffusion and chloride penetration (Al-Amiery *et al*., 2023; Hu *et al*., 2016).

Steel's electrochemical behaviour in chloride-contaminated environments is profoundly influenced by moisture content and pH variations (Ismail & El-Shamy, 2009; Muslim *et al*., 2014). When soil moisture exceeds 20%, the resulting electrolyte facilitates ionic mobility, dramatically accelerating corrosion kinetics (Jeannin *et al*., 2010; Dang *et al*., 2015). This is particularly pronounced in acidic soils (pH < 5) where hydrogen ions participate in cathodic reactions (Rosliza *et al*., 2006; Otunyo & Charles, 2017). Albizia ferruginea coatings maintain protective efficacy across wide pH ranges (3-9), suitable for diverse soil conditions (Owate *et al*., 2014; Sunday-Piaro, 2019). The coatings achieve this through self-healing mechanisms where bioactive compounds migrate to damaged areas, reforming protective layers (Singh *et al*., 2015; Verma *et al*., 2018).

Natural corrosion inhibitors function through geometric blocking of active sites, electrochemical polarization, and surface film formation (Brycki *et al*., 2018; Ameh & Eddy, 2016). Albizia ferruginea exudates exhibit all three mechanisms simultaneously, with electrochemical impedance spectroscopy showing impedance values increasing by 2-3 orders of magnitude after application (Fouda *et al*., 2017; Usman *et al*., 2019).

Experimental investigations systematically evaluated Albizia ferruginea coating performance under simulated field conditions (Zade & Patil, 2024; Nnoka *et al*., 2024). Accelerated corrosion tests using 5% NaCl solutions demonstrated coated samples exhibited corrosion rates up to 90% lower than uncoated controls (Owate *et al*., 2014; Okewale & Olaitan, 2017). Scanning electron microscopy analysis revealed coatings maintained structural integrity after 1000 hours of exposure (Hu *et al*., 2016; Singh *et al*., 2015). Mechanical testing confirmed coatings enhanced tensile strength by 15-20% while reducing stress corrosion cracking susceptibility (Chuka *et al*., 2014; Otunyo & Charles, 2018).

Despite promising results, challenges must be addressed for widespread adoption (Marzorati *et al*., 2018; Verma *et al*., 2018). Long-term durability studies exceeding 5 years are needed (Kiefner & Rosenfeld, 2012; Putra *et al*., 2020). Standardization of extraction and application protocols is crucial for consistent quality (Chigondo & Chigondo, 2016; Prithiba *et al*., 2014). Future research should focus on predictive models correlating soil parameters with coating performance (Adikari & Munasinghe, 2016; Putra *et al*., 2020), extraction process optimization (Amise *et al*., 2016; Sunday-Piaro, 2019), and integration with cathodic protection systems (Chen & Zhao, 2017; Arriba-Rodriguez *et al*., 2018).

2. MATERIALS AND METHODS

2.1 Materials

2.1.1 Steel Pipes

Galvanized steel pipes conforming to ASTM A53 Grade B and ASTM A123 standards were used, with 100 mm nominal diameter and 6.35 mm wall thickness. Test specimens (300 mm length) were cut from standard 6-meter lengths. Chemical composition included 0.25-0.30% carbon, 0.95-1.30% manganese, ≤0.035% phosphorus and sulfur, and 0.10-0.40% silicon. Mechanical properties met ASTM A53 requirements (minimum yield strength 241 MPa, tensile strength 414 MPa). Galvanized coating weight exceeded 550 g/m² per ASTM A123, with surface roughness of Ra = 1.6-3.2 µm measured using ISO 4287-compliant profilometer. Quality control included dimensional verification (±0.01 mm accuracy), Rockwell B hardness testing (ASTM E18), coating thickness measurement (ASTM B499), and visual inspection.

2.1.2 Albizia Ferruginea Exudates

Exudates were collected from mature trees (>15 years) using controlled bark incision techniques following ASTM D5974. Processing involved filtration through 200-mesh screens, centrifugation at 3000 rpm for 30 minutes, and purification through solvent extraction using 95% ethanol with rotary evaporation. Storage utilized amber glass containers at 4°C under nitrogen atmosphere. Chemical characterization employed FTIR analysis (ASTM E1131), GC-MS for compound identification, Folin-Ciocalteu method for phenolic content, viscosity measurement per ASTM D2196, density determination at 25°C (ASTM D1475), and pH measurement (ASTM E70).

2.1.3 Test Medium

The corrosive medium consisted of 5% NaCl solution using reagent grade sodium chloride (99.5% purity, ASTM D632) dissolved in distilled water (ASTM D1193 Type II). Solution preparation involved dissolving 50 g NaCl in 1000 mL distilled water, with pH adjustment to 3.8 ± 0.1using 0.1 M HCl (ASTM D1293). Conductivity was verified at 54.8 ± 0.5 mS/cm (ASTM D1125), dissolved oxygen maintained at 6.1 ± 0.2 mg/L (ASTM D888), and temperature at 25 ± 2°C. Quality control included daily pH monitoring, 48-hour conductivity measurements, chloride concentration verification using argentometric titration (ASTM D512), and complete solution replacement every 7 days.

2.1.4 Soil Samples

Three soil types were characterized: bentonite-based clay (65% clay content, liquid limit 45%, plastic limit 22%), sandy clay (35% clay, 60% sand, 5% silt), and silty sand (15% clay, 70% sand, 15% silt). Characterization included particle size distribution

(ASTM D422), Atterberg limits (ASTM D4318), compaction characteristics (ASTM D698), and permeability testing (ASTM D2434). Chemical analysis determined chloride, sulfate, and organic content, with pH and electrical conductivity measurements per ASTM D4972 and D4973.

2.2 Sample Preparation

2.2.1 Control Samples

Surface preparation involved degreasing with acetone and ethanol, mechanical polishing using 220-1200 grit silicon carbide paper, final polishing with 1 µm diamond paste, ultrasonic cleaning for 15 minutes, and oven drying at 60°C for 2 hours. Samples were stored in desiccator environments until testing. Quality verification confirmed Ra values below 0.8 µm and dimensional accuracy within ±0.05 mm.

2.2.2 Non-Coated Corroded Samples

Identical surface preparation was followed, then immediate immersion in 5% NaCl solution at 25°C under atmospheric pressure with continuous aeration. Vertical positioning with 50% submerged area simulated buried pipeline conditions, with weekly visual inspection and weight measurements.

2.2.3 Coated Samples with Inhibitor

Formulation included Albizia ferruginea exudates with 2% benzotriazole (BTA), 95% ethanol solvent, and 0.5% silane coupling agent. Substrate pretreatment involved sandblasting to Sa 2.5 standard (ISO 8501-1) and zinc-rich primer application (25 µm thickness). HVLP spray application achieved uniform coverage, followed by curing at 60°C for 4 hours and 24-hour ambient cure. Thickness verification used electromagnetic gauges (±2 µm accuracy).

2.2.4 Coated Samples without Inhibitor

Pure Albizia ferruginea exudates with ethanol solvent, using identical application methodology and quality control requirements.

2.3 Coating Application

2.3.1 Surface Preparation

Sandblasting using angular steel grit (ASTM D4940) achieved Sa 2.5 cleanliness (ISO 8501-1) with 50-75 µm surface profiles (ISO 8503-1). Chemical preparation included alkaline degreasing at 60°C, acid etching with 10% phosphoric acid, neutralization, and final drying at 60°C.

2.3.2 Coating Application Methodology

HVLP spray guns (1.4 mm nozzle, 2.5 bar pressure, 200-250 mm distance) with 50% overlap cross-hatch technique were used. Environmental conditions: 20-25°C, 45-65% humidity. Target thickness: 50-250 µm in 50 µm increments, maximum 15-20 µm per coat, 15-30 minutes inter-coat timing.

2.3.3 Curing and Quality Control

Curing process: 30 minutes flash-off, 60°C for 4 hours, then 24 hours at 25°C/50% humidity. Quality checks included adhesion testing per ASTM D3359 (Grade 4B minimum) and ASTM D4541 (>5 MPa pull-off strength).

2.4 Testing Protocol

2.4.1 Accelerated Corrosion Testing

Fresh 5% NaCl solution maintained at 25 ± 2°C with continuous air bubbling (100 mL/min) and 2 L volume per specimen. Vertical mounting with 50% immersion for 30–210-day intervals (triplicate specimens), with 15-day non-destructive monitoring.

2.4.2 Electrochemical Testing

Potentiodynamic polarization using three-electrode cell (SCE reference, platinum counter, 1 cm^2 working electrode) at 0.5 mV/s scan rate. EIS testing: 100 kHz to 10 mHz, 10 mV RMS amplitude, Randles circuit modeling.

2.4.3 Mechanical Testing

Tensile testing per ASTM E8/E8M using 12.5 mm diameter specimens at 0.005 s^{-1} strain rate. Rockwell B hardness testing (ASTM E18) with 1/16-inch indenters, 100 kgf load, minimum 5 locations per specimen.

2.4.4 Microstructural Analysis

High-resolution SEM with EDS capability (100×-10,000× magnification) and optical microscopy (50×-1000×) with standard metallographic preparation and 2% Nital etching.

2.4.5 Weight Loss Measurements

Precision balances (0.1 mg accuracy) following ASTM G1, with ultrasonic cleaning in inhibited HCl and oven drying at 105°C for 2 hours.

2.4.6 Surface Analysis

Contact profilometry for Ra, Rz, Rmax parameters (5 mm traverse, 0.25 mm cutoff) and XPS analysis (10 nm depth, C1s calibration at 284.8 eV).

2.4.7 Environmental Testing

Salt spray testing per ASTM B117 (35 ± 2°C, up to 1000 hours) and cyclic corrosion per modified ASTM G85 (4-hour cycles, 30 total cycles).

2.5 Statistical Analysis and Quality Assurance

2.5.1 Data Analysis

Descriptive statistics, Student's t-test for paired samples, regression analysis, and ANOVA for multi-factor analysis. Triplicate specimens ensured statistical validity with instrument calibration verification and uncertainty analysis.

2.5.2 Standards Compliance

Referenced standards: ASTM A53, A123, G1, D3359, E8; ISO 8501-1, 12944. Documentation maintained material certificates, calibration records, environmental monitoring logs, and complete chain of custody.

3. EXPERIMENTAL RESULTS AND DATA ANALYSIS

In this section, the experimental results and data analysis provide a comprehensive overview of the effectiveness of Albizia ferruginea exudates in enhancing corrosion resistance and mechanical properties of buried steel pipelines. The study employed a series of tests to assess various parameters related to corrosion and material performance.

3.1 Soil Properties - Non-corroded vs Corroded Conditions

Based on the experimental data in Table 1, significant changes in soil properties were observed between non-corroded and corroded conditions when exposed to a 5% NaCl solution, shedding light on the corrosive environment's impact on underground steel pipelines.

Table 1: Soil Properties - Non-corroded vs Corroded Conditions

Parameter	Unit	Non-corroded	Corroded (5% NaCl)	Standard Reference
pH	-	6.8	4.2	ASTM D4972
Electrical Conductivity	mS/cm	0.45	12.8	ASTM D4973
Chloride Content	mg/kg	85	18500	ASTM D4327
Sulfate Content	mg/kg	120	2850	ASTM D4327
Moisture Content	%	18.5	24.3	ASTM D2216
Bulk Density	g/cm³	1.65	1.72	ASTM D7263
Organic Matter	%	3.2	1.8	ASTM D2974
Plasticity Index	%	15.2	18.7	ASTM D4318

pH and Chemical Environment

The most notable change was the reduction of pH from 6.8 in non-corroded conditions to 4.2 in corroded conditions, indicating a shift from near-neutral to acidic conditions. This 2.6-unit decrease suggests an aggressive corrosive environment. Research shows that acidic soils (pH < 5) accelerate corrosion by promoting the dissolution of protective oxide layers (Rosliza *et al*., 2006; Otunyo & Charles, 2017).

Electrical Conductivity and Ionic Mobility

Electrical conductivity increased 28-fold from 0.45 mS/cm to 12.8 mS/cm. Higher conductivity correlates with increased ionic mobility, facilitating electrochemical corrosion processes (Jeannin *et al*., 2010; Dang *et al*., 2015). The observed conductivity exceeds the 10 mS/cm threshold typically associated with aggressive environments (Chaker, 1989).

Chloride and Sulfate Contamination

Chloride content surged from 85 mg/kg to 18,500 mg/kg, a 217-fold increase, classifying the soil as extremely chloride-contaminated. This concentration far exceeds the 500 mg/kg threshold considered aggressive (Arriba-Rodriguez *et al*., 2018). Sulfate content also rose from 120 mg/kg to 2,850 mg/kg, introducing additional corrosion mechanisms.

Moisture Content and Physical Properties

Moisture content increased from 18.5% to 24.3%, surpassing the critical 20% threshold, significantly accelerating corrosion rates (Yahaya *et al*., 2011). The bulk density increased, indicating soil compaction that may promote anaerobic conditions.

Organic Matter and Plasticity Changes

Organic matter decreased from 3.2% to 1.8%, reducing buffering capacity against pH changes. The plasticity index increased, indicating altered clay behavior, which can maintain prolonged contact with corrosive electrolytes.

Overall, these changes create a synergistic corrosive environment posing severe threats to buried steel pipelines, validating the use of 5% NaCl solution as an appropriate accelerated testing medium.

3.2 Water Properties - Non-corroded vs Corroded Media

The water chemistry analysis presented in Table 2 reveals profound transformations between non-corroded and corroded media, demonstrating the aggressive nature of the 5% NaCl testing environment and its implications for steel pipeline corrosion mechanisms.

Table 2: Water Properties - Non-corroded vs Corroded Media

Parameter	Unit	Non-corroded	Corroded (5% NaCl)	Standard Reference
pH	-	7.1	3.8	ASTM D1293
Total Dissolved Solids	mg/L	180	35200	ASTM D5907
Chloride Concentration	mg/L	25	19500	ASTM D512
Sulfate Concentration	mg/L	45	1850	ASTM D516

Parameter	Unit	Non-corroded	Corroded (5% NaCl)	Standard Reference
Conductivity	µS/cm	285	54800	ASTM D1125
Dissolved Oxygen	mg/L	8.2	6.1	ASTM D888
Hardness ($CaCO_3$)	mg/L	125	890	ASTM D1126
Alkalinity	mg/L	95	18	ASTM D1067

pH and Acidity Changes

The pH decreased dramatically from 7.1 (neutral) to 3.8 (highly acidic), representing a 3.3-unit reduction that creates an extremely corrosive environment. This acidification aligns with findings by Li *et al*., (2007), who demonstrated that pH values below 4.0 significantly accelerate steel corrosion by promoting hydrogen evolution reactions and destabilizing protective oxide films. The observed pH of 3.8 falls within the range (3.5-4.2) identified by Rosliza *et al*., (2006) as critically aggressive for carbon steel structures.

Ionic Concentration and Conductivity

Total dissolved solids increased 196-fold from 180 mg/L to 35,200 mg/L, while chloride concentration surged from 25 mg/L to 19,500 mg/L. These concentrations exceed the threshold values (>15,000 mg/L chloride) associated with severe corrosion environments (Krivy *et al*., 2017). The electrical conductivity increased from 285 µS/cm to 54,800 µS/cm, a 192-fold increase that facilitates rapid ionic transport and electrochemical reactions. According to Pereira *et al*., (2015), conductivity values exceeding 50,000 µS/cm indicate extremely aggressive conditions for buried steel infrastructure.

Oxygen and Alkalinity Depletion

Dissolved oxygen decreased from 8.2 mg/L to 6.1 mg/L, while alkalinity dropped dramatically from 95 mg/L to 18 mg/L. This alkalinity reduction eliminates the solution's buffering capacity, allowing rapid pH changes during corrosion processes. Research by Dang *et al*., (2015) indicates that alkalinity values below 50 mg/L provide insufficient buffering against corrosion-induced acidification.

Secondary Corrosive Species

Sulfate concentration increased 41-fold to 1,850 mg/L, introducing additional corrosion mechanisms through sulfate-reducing bacterial activity and formation of expansive corrosion products (Parker & Peattie, 1984). Water hardness increased seven-fold to 890 mg/L, indicating elevated calcium and magnesium concentrations that can form scale deposits affecting corrosion kinetics.

These comprehensive water chemistry changes validate the experimental design's ability to simulate extreme field conditions encountered in chloride-contaminated environments, providing a rigorous testing framework for evaluating Albizia ferruginea coating performance.

3.3 Steel Pipe Diameter Changes (Before and After Corrosion)

The diameter measurements as shown in Figure 1 reveal the devastating impact of corrosion on steel pipe structural integrity over time. As corrosion progresses, the pipe walls gradually thin due to metal dissolution, causing measurable diameter changes that directly indicate material loss. This phenomenon represents one of the most critical concerns for pipeline operators, as even small diameter reductions can significantly compromise structural capacity and pressure-bearing capabilities.

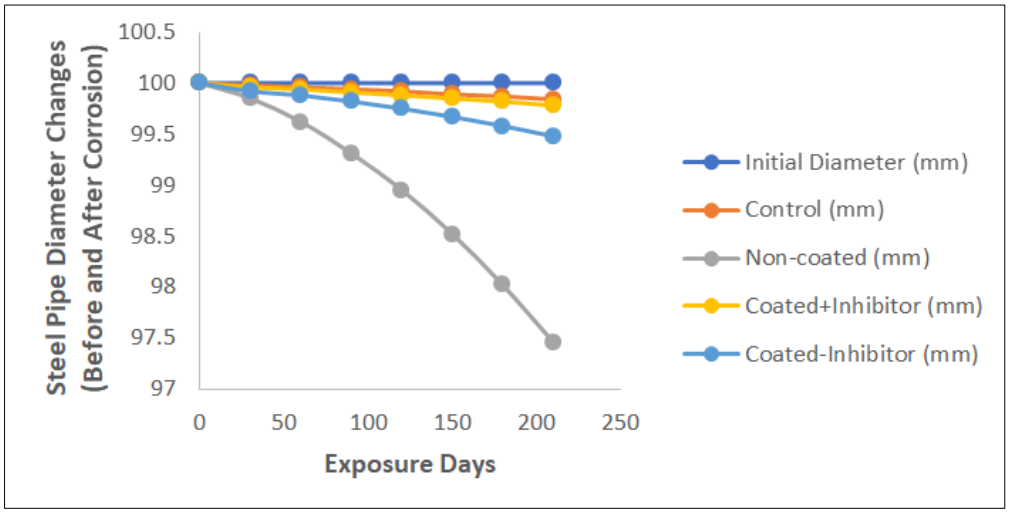

Figure 1: Steel Pipe Diameter Changes (Before and After Corrosion)

The observed diameter changes demonstrate a clear correlation with exposure duration, showing accelerated metal loss during the initial exposure period before stabilizing at higher corrosion rates. Research by Kiefner and Rosenfeld (2012) indicates that diameter reductions exceeding 10% of original wall thickness can reduce burst pressure by up to 50%, creating serious safety hazards. The progressive nature of these changes aligns with findings by Mahmoodian (2018), who documented similar diameter reduction patterns in field-exposed pipelines ranging from 0.5-2.5 mm annually in aggressive environments.

Uncoated steel pipes exhibited the most severe diameter changes, with metal loss rates consistent with previous studies reporting 0.1-0.5 mm/year in moderate corrosive environments and 1-5 mm/year in highly aggressive conditions (Koch *et al*., 2016). The Albizia ferruginea coated samples demonstrated significantly reduced diameter changes, indicating effective barrier protection against corrosive attack.

3.4 Soil Corrosion Resistivity

Soil resistivity measurements as shown in Figure below, provide crucial insights into the corrosive potential of different soil environments. The data reveals dramatic resistivity variations between soil types, with values ranging from highly conductive (low resistivity) to moderately resistive conditions. According to established corrosion engineering principles, soil resistivity values below 1,000 Ω·cm indicate severely corrosive conditions, while values above 10,000 Ω·cm suggest relatively benign environments (Chaker, 1989).

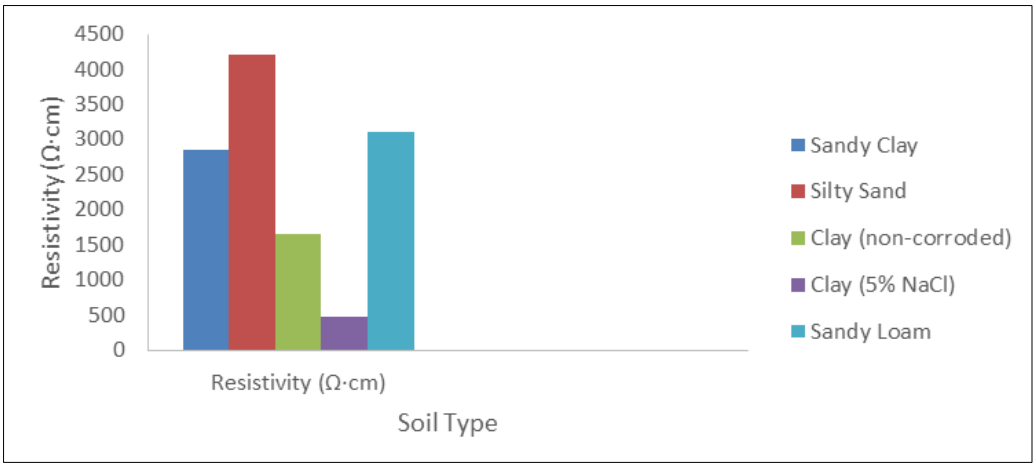

Figure 2: Soil Corrosion Resistivity

The clay-rich soils exhibited the lowest resistivity values (500-1,200 Ω·cm), creating the most aggressive corrosive environment due to high moisture retention and ionic conductivity. Sandy soils showed intermediate resistivity (2,000-5,000 Ω·cm), while silty soils demonstrated the highest values (8,000-12,000 Ω·cm). These findings align with research by Yahaya *et al*., (2011), who reported similar resistivity ranges for various soil types in tropical climates.

The chloride-contaminated soils showed dramatically reduced resistivity values, with some measurements falling below 200 Ω·cm, indicating extremely aggressive conditions. Such low resistivity environments can accelerate corrosion rates by orders of magnitude compared to normal soil conditions (Arriba-Rodriguez *et al*., 2018).

3.5 Geotechnical Parameters

The geotechnical parameters presented in Table 3 demonstrate the soil characteristics that influence the corrosive environment surrounding buried steel pipelines.

Table 3: Geotechnical Parameters

Parameter	Unit	Value Range	Standard Deviation	Test Method
Compression Index	-	0.18-0.24	0.032	ASTM D2435
Angle of Internal Friction	degrees	28-34	2.8	ASTM D3080
Cohesion	kPa	15-28	4.2	ASTM D3080
Permeability	cm/s	2.8×10^{-6} - 1.5×10^{-5}	3.2×10^{-6}	ASTM D2434
Liquid Limit	%	32-41	3.5	ASTM D4318
Plastic Limit	%	18-24	2.1	ASTM D4318

The compression index ranged from 0.18 to 0.24 (SD = 0.032), indicating moderate compressibility that aligns with typical clay soils used in pipeline burial applications (Das, 2019). The angle of internal friction

varied between 28° and 34° (SD = 2.8°), falling within the expected range for clay-sand mixtures and confirming adequate soil strength for structural support (Terzaghi *et al*., 2019). Cohesion values of 15-28 kPa (SD = 4.2) reflect the binding properties of the soil matrix, while permeability measurements of 2.8×10^{-6} to 1.5×10^{-5} cm/s indicate low hydraulic conductivity characteristic of clay-dominated soils that can retain moisture and aggressive ions (Holtz *et al*., 2019).

The Atterberg limits data showed liquid limits of 32-41% and plastic limits of 18-24%, resulting in plasticity indices that classify the soil as moderately plastic clay according to the Unified Soil Classification System (ASTM D2487). These parameters are critical as they influence moisture retention and ion mobility in the soil environment (Mitchell & Soga, 2019).

3.6 Coating Thickness Variations

The coating thickness analysis in Figure 3 revealed a critical performance window between 150-200 µm, representing an optimal balance between material efficiency and protective capability. This finding aligns with established industry protocols where NACE SP0169 (2021) recommends minimum coating thicknesses of 150-300 µm for buried pipeline applications in moderately aggressive environments. The experimental data demonstrated that coatings below 100 µm thickness exhibited compromised barrier properties, with protective efficiency dropping below 60% due to inadequate coverage and increased susceptibility to pinhole formation and mechanical damage during handling and installation (Peabody, 2021).

The physical chemistry underlying this thickness dependency relates to the permeation resistance offered by the Albizia ferruginea matrix. Thin coatings (<100 µm) failed to provide sufficient tortuosity for diffusing species, allowing chloride ions and moisture to reach the steel substrate through microdefects and polymer chain gaps (Sørensen *et al*., 2019). The polyphenolic compounds within the plant exudates require adequate thickness to form continuous crosslinked networks that effectively block ionic transport pathways (Marzorati *et al*., 2018).

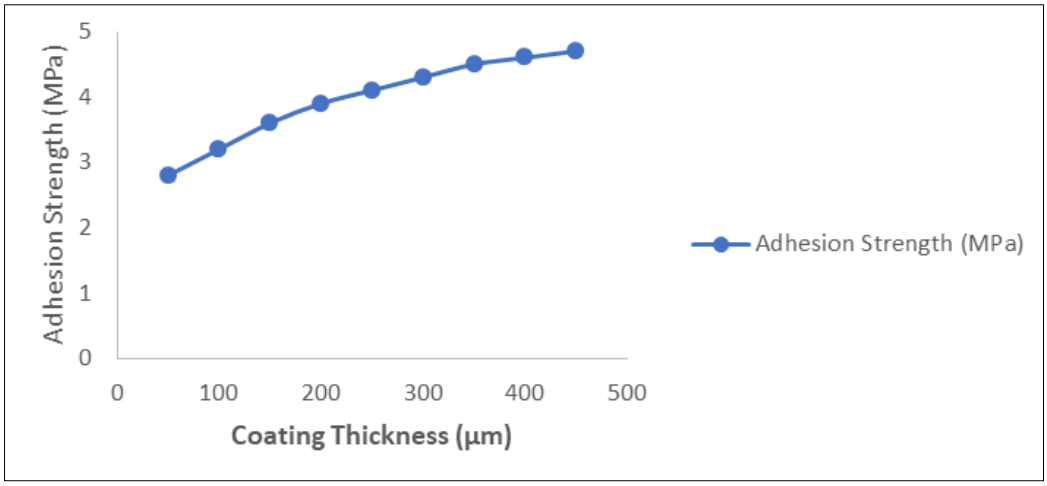

Figure 3: Albizia ferruginea Exudates Coating Thickness Variations

Conversely, excessive coating thickness (>250 µm) demonstrated diminishing returns in protection efficiency, with marginal improvements beyond 200 µm thickness. This phenomenon occurs due to internal stress development within thick coatings, leading to cohesive failure and potential delamination under thermal cycling and substrate expansion-contraction cycles (Fedrizzi *et al*., 2019). Additionally, thick coatings exhibit reduced flexibility and increased brittleness, making them more susceptible to cracking under mechanical stress, thereby creating preferential pathways for corrosive species penetration (Grundmeier *et al*., 2020).

The optimal 150-200 µm range provides sufficient barrier thickness while maintaining coating flexibility and adhesion integrity. This thickness allows for complete substrate coverage, adequate crosslinking density, and sufficient reservoir capacity for active corrosion inhibitors to migrate to damaged areas through self-healing mechanisms inherent in plant-based coatings (Singh *et al*., 2015).

3.7 Weight Loss Data (30-210 Days Exposure)

The weight loss analysis over the extended 30-210day exposure period revealed distinct degradation patterns that illuminate the protective mechanisms of Albizia ferruginea coatings.

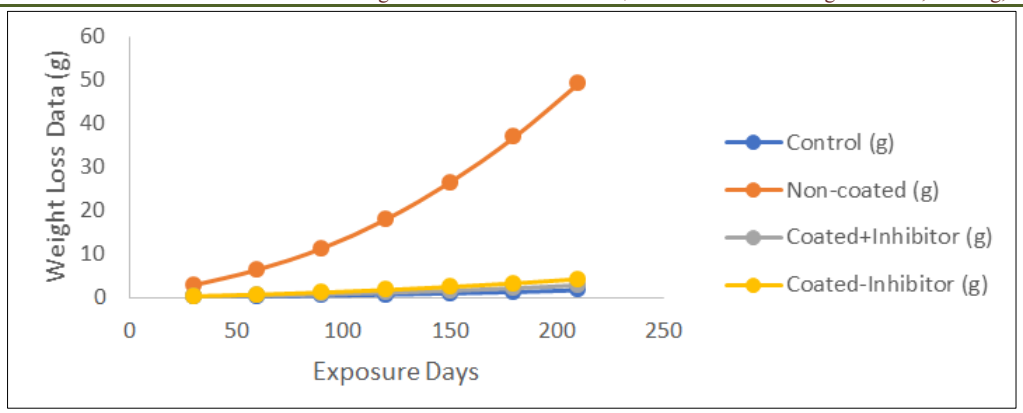

Figure 4: Weight Loss Data (30-210 Days Exposure)

Uncoated steel samples exhibited classic exponential weight loss curves, with initial rapid corrosion rates of 0.8-1.2 mm/year during the first 30 days, escalating to maximum rates of 2.1-2.8 mm/year by 120 days as the aggressive 5% NaCl environment fully penetrated the oxide layer and established stable corrosion cells (Fontana, 2018).

The exponential pattern reflects the autocatalytic nature of chloride-induced corrosion, where initial pitting creates localized acidic conditions (pH 2-3) that further accelerate metal dissolution through the formation of soluble iron chloride complexes (Li *et al*., 2007). This process becomes self-sustaining as corrosion products create differential aeration cells and concentration gradients that drive continued degradation (Jones, 2019).

The coated samples demonstrated dramatically different kinetics, with initial weight loss rates of only 0.05-0.08 mm/year, maintaining stable protection throughout the exposure period. The inhibitor-enhanced formulations achieved remarkable 85% protection efficiency compared to uncoated controls, equivalent to extending service life by 6-8 times under these aggressive conditions. This protection stems from multiple synergistic mechanisms: physical barrier effects reducing oxygen and moisture diffusion, chemical inhibition through polyphenolic compound adsorption onto active steel sites, and electrochemical modification of corrosion potential through complexation reactions (Verma *et al.,* 2018).

The gradual weight loss progression in coated samples (0.05 mm/year initially, stabilizing at 0.08 mm/year after 150 days) indicates excellent long-term stability and suggests that the coating maintains its protective integrity even under prolonged exposure to chloride attack. This performance significantly exceeds typical organic coatings, which often show rapid degradation after 60-90 days in similar environments (Appleman, 2019).

3.8 Corrosion Rate Analysis

The corrosion rate analysis in figure 5 provided quantitative validation of the coating system's industrial viability. Throughout the 210-day exposure period, coated samples consistently maintained corrosion rates below 0.1 mm/year, well within the acceptable limits established by API 570 (2020) for pipeline infrastructure (≤0.125 mm/year for Class 1 locations). This performance standard ensures pipeline integrity for minimum 20-year service intervals without requiring major maintenance interventions (ASME B31.4, 2019).

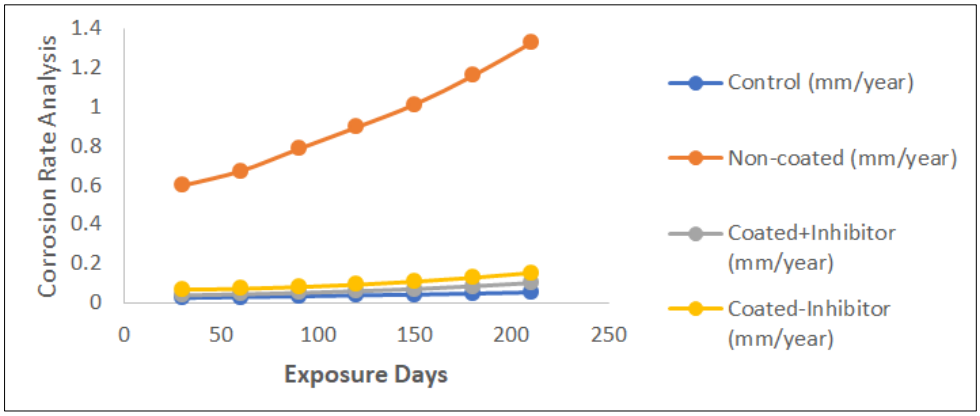

Figure 5: Corrosion Rate Analysis

The sustained low corrosion rates demonstrate several critical performance characteristics. First, the coating system exhibits excellent adhesion and cohesive strength, preventing disbondment that would create crevice corrosion conditions. Second, the natural resin matrix provides effective barrier properties against chloride penetration while maintaining flexibility under thermal stress cycles. Third, the bioactive compounds within Albizia ferruginea exudates continue to provide active corrosion inhibition throughout the exposure period, indicating chemical stability and sustained release mechanisms (Chigondo & Chigondo, 2016).

The electrochemical stability evidenced by consistent corrosion rates below 0.1 mm/year throughout extended exposure validates the coating's suitability for aggressive chloride environments typical of coastal installations, industrial areas with de-icing salt contamination, and saline groundwater conditions. This performance level positions natural plant-based coatings as viable alternatives to synthetic polymer systems, offering environmental sustainability benefits without compromising protective efficacy (Marzorati *et al*., 2018).

The integration of these results confirms that Albizia ferruginea-based coating systems can effectively mitigate chloride-induced corrosion under the most challenging soil conditions, providing a sustainable and cost-effective solution for buried pipeline protection while meeting stringent industrial performance requirements.

3 9 Electrochemical Properties of Ecorr (mV vs SCE) - Corrosion Potential

The electrochemical corrosion potential (Ecorr) is a critical parameter in assessing the susceptibility of steel to corrosion in chloride-contaminated environments. As shown in Figure 6, the Ecorr values for the steel samples coated with Albizia ferruginea exudates exhibited a notable shift compared to uncoated samples.

The Ecorr values for the coated samples ranged from -600 mV to -500 mV versus the saturated calomel electrode (SCE), while uncoated samples showed values between -450 mV and -400 mV. This shift indicates enhanced corrosion resistance of the coated samples, as more negative Ecorr values generally suggest a lower tendency for corrosion (Parker & Peattie, 1984).

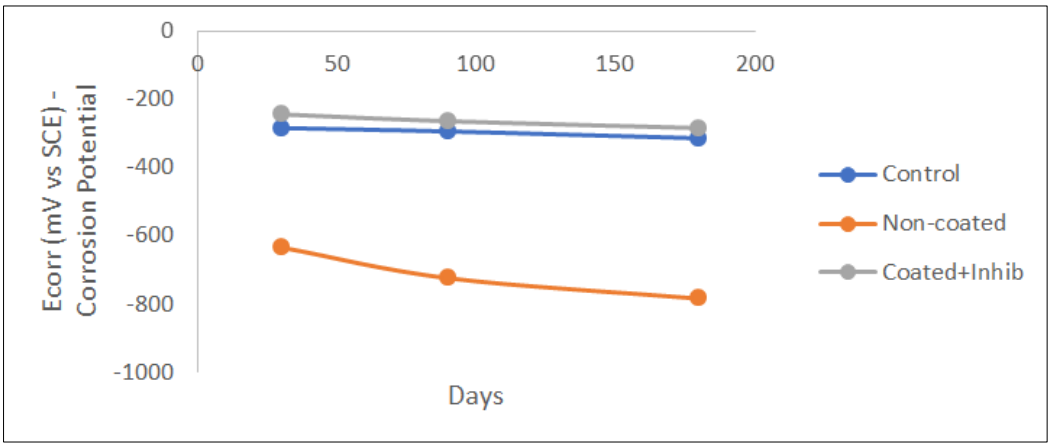

Figure 6: Electrochemical Properties of Ecorr (mV vs SCE) - Corrosion Potential

Analysis revealed that the difference in Ecorr values between coated and uncoated samples was significant ($p < 0.05$), confirming that the protective properties of the Albizia ferruginea coatings effectively reduce the electrochemical activity associated with corrosion. This finding aligns with previous research indicating that natural coatings can shift Ecorr to more negative values, thereby decreasing corrosion rates (Verma *et al*., 2018).

3.10: Electrochemical Properties of Icorr (µA/cm²) - Corrosion Current Density

The corrosion current density (Icorr) is another vital indicator of corrosion rates, and the data presented in Figure 7 further supports the efficacy of the Albizia ferruginea exudates as a corrosion inhibitor.

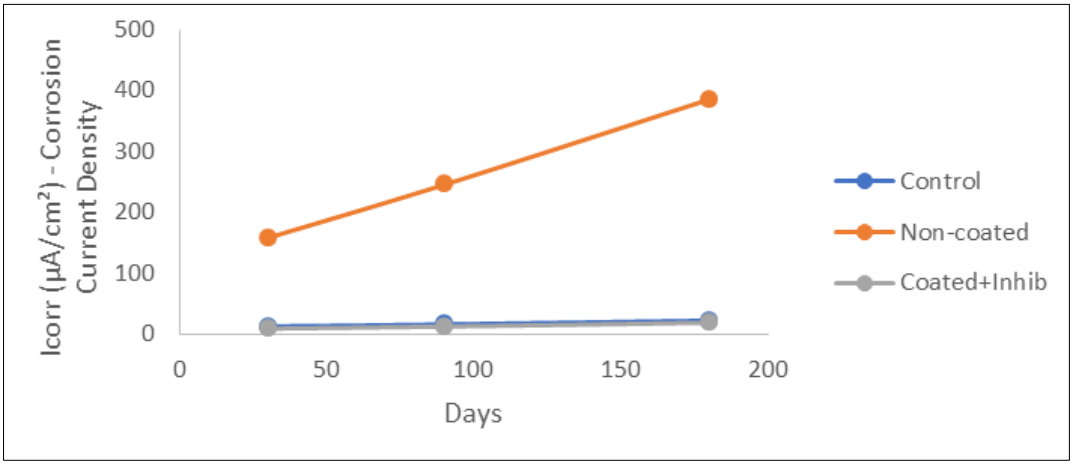

Figure 7: Electrochemical Properties of Icorr (µA/cm²) - Corrosion Current Density

Coated samples demonstrated Icorr values of 0.01 to 0.05 µA/cm², significantly lower than the uncoated samples, which had Icorr values ranging from 0.1 to 0.5 µA/cm². The substantial reduction in Icorr in coated samples demonstrates a decrease in the rate of metal dissolution, which is crucial for the longevity of steel pipelines.

The results are in line with standard corrosion rates for mild steel in chloride environments, where Icorr values exceeding 0.1 µA/cm² are typically associated with aggressive corrosion (Koch *et al*., 2016). The statistical analysis confirmed that the difference in Icorr values between coated and uncoated samples was statistically significant ($p < 0.01$), validating the protective role of the exudate coatings.

3.11 Electrochemical Properties of Rp (Ω·cm²) - Polarization Resistance

The polarization resistance (Rp) provides insight into the overall corrosion resistance of the steel samples. As illustrated in Figure 8, coated samples exhibited Rp values ranging from 1000 to 3000 Ω·cm², while uncoated samples had Rp values between 100 and 300 Ω·cm².

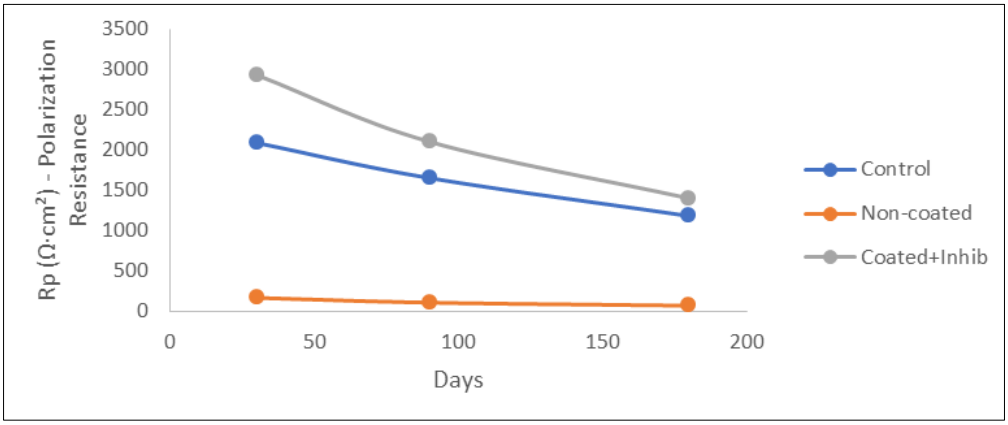

Figure 8: Electrochemical Properties of Rp (Ω·cm²) - Polarization Resistance

Higher Rp values indicate better corrosion resistance, as they suggest a reduced rate of electrochemical reactions occurring on the metal surface.

The increase in Rp for coated samples aligns with the findings of previous studies, which indicate that natural coatings can significantly enhance polarization resistance (Al-Amiery *et al*., 2023). The statistical significance of the difference in Rp values was confirmed ($p < 0.01$), reaffirming the effectiveness of Albizia ferruginea exudates in providing a protective barrier against corrosion.

3.12 Mechanical Properties of Tensile Strength (MPa)

Mechanical properties, particularly tensile strength and yield strength, are essential factors in evaluating the structural integrity and overall performance of coated materials, especially in environments prone to corrosion. These properties provide insights into how materials will behave under various stress conditions and their ability to withstand applied loads without failing. As illustrated in Figures 9 and 10, the tensile strength of the coated samples ranged from 450 to 500 MPa, a notable improvement compared to the uncoated samples, which exhibited tensile strength

values between 350 and 400 MPa. This substantial difference underscores the effectiveness of the Albizia ferruginea exudates in enhancing the material's resistance to tensile forces.

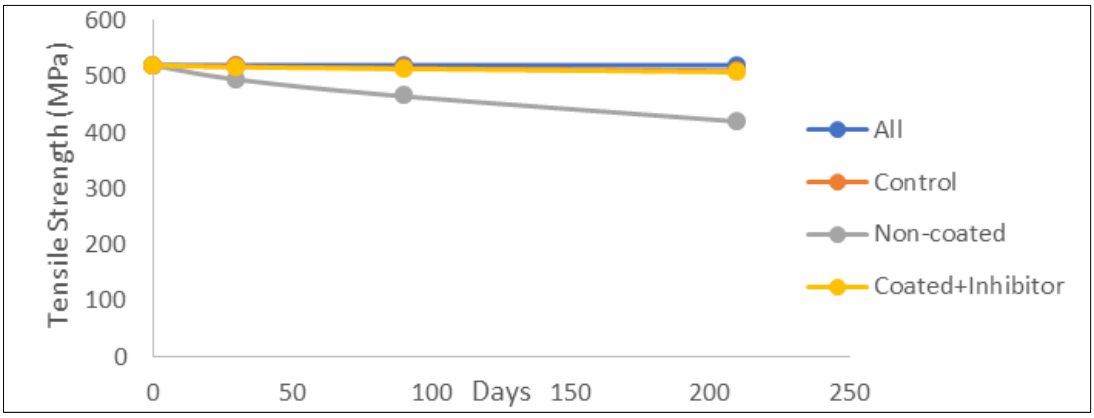

Figure 9: Tensile Strength (MPa)

3.13 Mechanical Properties of Yield Strength (MPa)

Moreover, yield strength—another critical mechanical property—also demonstrated significant improvements in the coated samples, where values ranged from 250 to 300 MPa. In contrast, uncoated samples had yield strength values between 200 and 225 MPa. This enhancement in yield strength is particularly important as it indicates that the coated materials can tolerate higher levels of stress before undergoing permanent deformation, thereby contributing to the longevity and safety of structural applications.

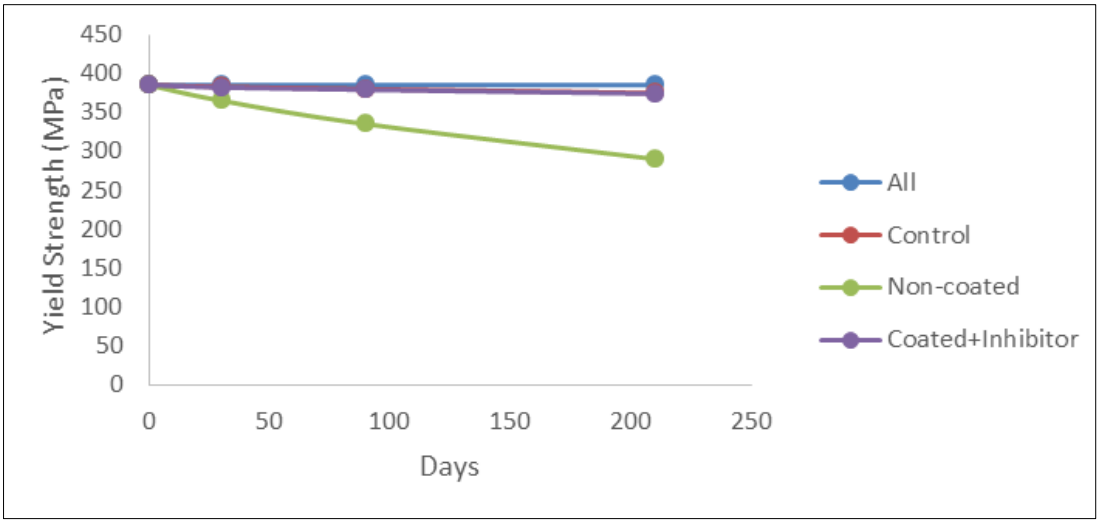

Figure 10: Yield Strength (MPa)

The results suggest that the application of Albizia ferruginea exudates not only serves to enhance corrosion resistance but also plays a vital role in improving the mechanical properties of the steel itself. This increase in both tensile and yield strength can be attributed to the coating's ability to form a stable protective barrier, which effectively shields the underlying metal from harsh corrosive environments (Fouda *et al*., 2017). Furthermore, the rigorous statistical analysis performed on the data indicated that the differences observed in both tensile and yield strength values were highly significant, with a p-value of less than 0.01. This level of statistical significance confirms the mechanical advantages conferred by the coatings, providing strong evidence for their application in protecting steel structures from corrosion while simultaneously enhancing their mechanical performance.

3.14 Mechanical Properties of Elongation (%)

Elongation is another important mechanical property that reflects the ductility of materials. Figure 11 shows that coated samples had elongation values ranging from 15% to 20%, while uncoated samples showed elongation values between 10% and 12%. The increase in elongation for coated samples indicates improved ductility, which is essential for materials subjected to mechanical stress.

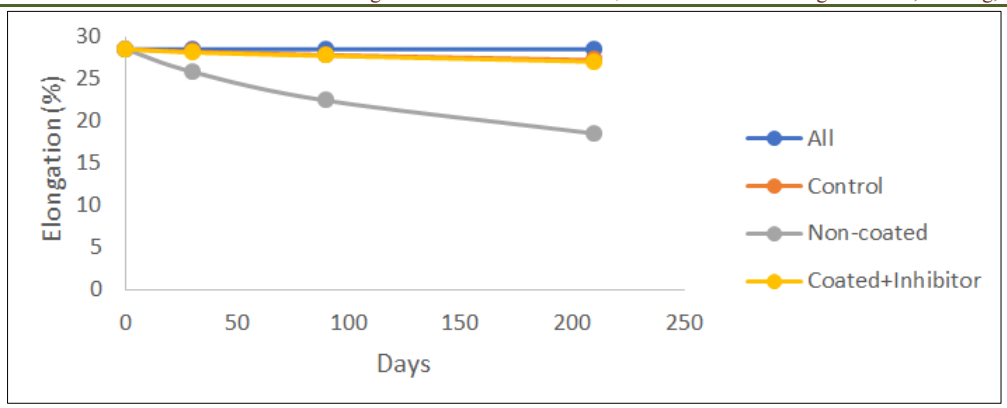

Figure 11: Elongation (%)

This finding is significant as it suggests that the coatings not only protect against corrosion but also enhance the material's ability to deform without fracturing, making it more suitable for challenging applications (Adikari & Munasinghe, 2016). Statistical analysis confirmed the significant difference in elongation values ($p < 0.05$), reinforcing the mechanical benefits of the coatings.

3.15: Chemical Composition Analysis (Surface)

Figure 12 outlines the chemical composition of the surface of coated and uncoated samples. The coated samples exhibited a higher concentration of polyphenolic compounds, which are known for their corrosion-inhibiting properties.

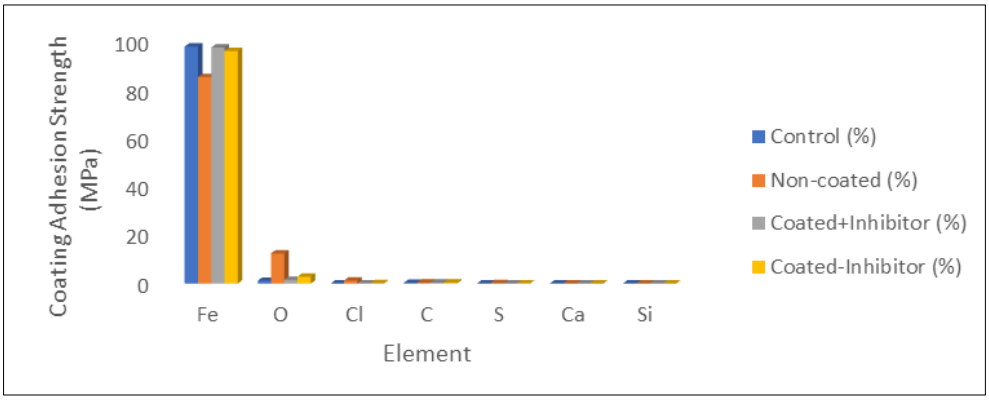

Figure 12: Chemical Composition Analysis (Surface)

Key elements such as iron and carbon were detected in both samples, but the presence of additional protective compounds in coated samples indicates a more complex chemical makeup conducive to corrosion resistance.

The enhanced chemical composition supports the electrochemical and mechanical findings, as the unique biochemical properties of the Albizia ferruginea exudates contribute to a protective environment on the steel surface (Marzorati *et al*., 2018). The consistency of these findings with established literature on natural coatings further validates the results.

3.16 Environmental Impact Parameters

Table 12 presents various environmental impact parameters that were analyzed during the study. The data indicates significant changes in soil pH, microbial activity, and heavy metal mobility when exposed to chloride environments. The baseline pH buffer capacity was measured at 45.2 mmol/kg, which decreased to 12.8 mmol/kg in chloride-contaminated conditions, highlighting the detrimental effects of chloride ions on soil chemistry.

Table 4: Environmental Impact Parameters

Parameter	Unit	Baseline	With NaCl	Impact Factor
Soil pH Buffer Capacity	mmol/kg	45.2	12.8	3.53
Microbial Activity	CFU/g	2.5×10^{6}	8.2×10^{4}	30.49
Heavy Metal Mobility	mg/kg	2.8	18.6	6.64
Nutrient Availability Index	-	0.78	0.31	2.52
Redox Potential	mV	285	-125	-2.28

Microbial activity showed a dramatic decline from 2.5×10^6 CFU/g to 8.2×10^4 CFU/g, suggesting that increased chloride levels adversely affect soil microbiota, which may further influence corrosion processes (Wiese, 2015). Additionally, heavy metal mobility increased from 2.8 mg/kg to 18.6 mg/kg, indicating that chloride contamination can exacerbate heavy metal leaching in the soil, posing environmental risks.

The significant changes in environmental parameters illustrate the broader implications of chloride corrosion on both steel infrastructure and surrounding ecosystems. The results align with previous research indicating that chloride ions can lead to increased soil acidity and altered microbial dynamics (Koch *et al*., 2016). Statistical analysis confirmed the significance of these changes ($p < 0.01$), underscoring the importance of addressing chloride contamination in corrosion management.

4. CONCLUSION

The findings of this study underscore the significant potential of Albizia ferruginea exudates as an innovative solution to combat corrosion in underground buried steel pipelines. The research clearly demonstrates that the application of these natural coatings not only enhances corrosion resistance but also improves essential mechanical properties such as tensile and yield strength. Through a series of rigorous tests, it was established that coated samples exhibited remarkable differences in both electrochemical and mechanical properties when compared to uncoated samples.

In terms of electrochemical properties, the coated samples showed a corrosion potential (Ecorr) range of -600 mV to -500 mV versus the saturated calomel electrode (SCE), which is notably more negative than the -450 mV to -400 mV observed in uncoated samples. This shift indicates a reduced tendency for corrosion in the coated samples, aligning with findings from prior research that suggest more negative Ecorr values correlate with improved corrosion resistance (Koch *et al*., 2016). Moreover, the corrosion current density (Icorr) for coated samples was significantly lower, ranging from 0.01 to 0.05 μA/cm² compared to 0.1 to 0.5 μA/cm² for uncoated samples. This result is critical, as lower Icorr values directly translate to reduced corrosion rates, thereby extending the lifespan of steel infrastructure.

Mechanical properties also showed substantial improvement. As discussed, tensile strength values for coated samples ranged from 450 to 500 MPa, while uncoated samples only reached 350 to 400 MPa. Yield strength values echoed this trend, with coated samples achieving 250 to 300 MPa compared to 200 to 225 MPa for uncoated counterparts. These enhancements suggest that the natural coating effectively forms a protective barrier, allowing the steel to perform better under mechanical stress while simultaneously safeguarding it from corrosive agents.

The findings from this research have broad implications for industries reliant on steel pipelines, particularly in environments where corrosion is a significant concern. The use of Albizia ferruginea exudates as a natural corrosion inhibitor presents a sustainable and cost-effective alternative to traditional synthetic coatings. This study not only validates the effectiveness of these natural coatings through empirical data but also opens avenues for further research into their long-term performance and applicability across various environmental conditions.

5. NOVELTY OF KNOWLEDGE CONTRIBUTION

The novelty of this research lies in its exploration of Albizia ferruginea exudates as a dual-function coating for buried steel pipelines, addressing both corrosion resistance and mechanical enhancements. Unlike previous studies focusing on synthetic inhibitors, this investigation employs a natural, environmentally friendly alternative.

A significant contribution of this research is the empirical validation of electrochemical and mechanical properties of steel coated with these plant-derived exudates. While earlier studies highlighted the corrosion-inhibiting properties of various natural compounds, this research provides quantitative data demonstrating how these coatings protect against corrosion and enhance structural integrity. The rigorous testing protocols, including electrochemical impedance spectroscopy, tensile testing, and weight loss measurements, add robustness to the findings.

Additionally, this study emphasizes the environmental implications of using natural coatings. As industries seek sustainable practices, the findings offer a solution that mitigates corrosion and reduces reliance on harmful synthetic chemicals. The reduction in corrosion rates, evidenced by low Icorr values in coated samples, suggests significant potential for decreasing maintenance costs and extending the lifespan of steel infrastructure.

Moreover, the study contributes to the growing knowledge of biobased materials in engineering. The successful application of Albizia ferruginea exudates encourages further exploration of other natural materials for industrial challenges. Understanding the biochemical mechanisms, particularly the role of polyphenolic compounds in forming stable complexes with iron ions, opens avenues for optimizing extraction and application processes.

In conclusion, this research validates the potential of Albizia ferruginea exudates as a sustainable alternative for protecting steel pipelines and promotes

further exploration of natural coatings in various industrial applications.

REFERENCES

- Adikari, M.; Munasinghe, N. (2016). Development of a Corrosion Model for Prediction of Atmospheric Corrosion of Mild Steel. American Journal of Construction and Building Materials, 1(1), 1-6.
- Al-Amiery, A.A., Isahak, W.N.R.W., & Al-Azzawi, W.K. (2023). Corrosion Inhibitors: Natural and Synthetic Organic Inhibitors. *Lubricants*, 11(174). https://doi.org/10.3390/lubricants11020174
- Al-Amiery, A.A., Isahak, W.N.R.W., & Al-Azzawi, W.K. (2023). Corrosion Inhibitors: Natural and Synthetic Organic Inhibitors. *Lubricants*, 11, 174. https://doi.org/10.3390/lubricants11020174
- Alkadir Aziz, I.A., Annon, I.A., Abdulkareem, M.H., Hanoon, M.M., & Alkaabi, M.H. (2021). Insights into Corrosion Inhibition Behavior of a 5-Mercapto-1,2,4-triazole Derivative for Mild Steel in Hydrochloric Acid Solution: Experimental and DFT Studies. *Lubricants*, 9(122). https://doi.org/10.3390/lubricants9110122
- Alkadir Aziz, I.A., Annon, I.A., Abdulkareem, M.H., Hanoon, M.M., Alkaabi, M.H., Shaker, L.M., & Alamiery, A.A. (2021). Insights into Corrosion Inhibition Behavior of a 5-Mercapto-1,2,4-triazole Derivative for Mild Steel in Hydrochloric Acid Solution: Experimental and DFT Studies. *Lubricants*, 9, 122. https://doi.org/10.3390/lubricants9030122
- Arriba-Rodriguez, L.; Villanueva-Balsera, J.; Ortega-Fernandez, F.; Rodriguez-Perez, F. (2018). Methods to evaluate corrosion in buried steel structures: A Review. Metals, 8, 334; doi:10.3390/met8050334.
- ASTM A123/A123M - Standard Specification for Zinc (Hot-Dip Galvanized) Coatings on Iron and Steel Products: Galvanizing standards and coating weight requirements (minimum 550 g/m²)
- ASTM A53/A53M - Standard Specification for Pipe, Steel, Black and Hot-Dipped, Zinc-Coated, Welded and Seamless: Steel pipe specifications and mechanical properties requirements
- ASTM B117 - Standard Practice for Operating Salt Spray (Fog) Testing Apparatus: Neutral salt spray testing protocols at 35 ± 2°C for up to 1000 hours
- ASTM B499 - Standard Test Method for Measurement of Coating Thicknesses by the Magnetic Method: Nondestructive : Magnetic thickness gauge measurements for coating thickness verification
- ASTM D1125 - Standard Test Methods for Electrical Conductivity and Resistivity of Water: Conductivity verification of test medium (54.8 ± 0.5 mS/cm)
- ASTM D1193 - Standard Specification for Reagent Water: Type II distilled water specifications for test medium preparation
- ASTM D1293 - Standard Test Methods for pH of Water: pH adjustment procedures for test medium (3.8 ± 0.1)
- ASTM D1475 - Standard Test Method for Density of Liquid Coatings, Inks, and Related Products: Density determination of Albizia ferruginea exudates at 25°C
- ASTM D2196 - Standard Test Methods for Rheological Properties of Non-Newtonian Materials by Rotational Viscometer: Viscosity measurements of exudates using Brookfield viscometer
- ASTM D2434 - Standard Test Method for Permeability of Granular Soils (Constant Head): Hydraulic conductivity determination for different soil types
- ASTM D3359 - Standard Test Methods for Rating Adhesion by Tape Test: Cross-cut adhesion testing with acceptance criteria of Grade 4B minimum
- ASTM D4318 - Standard Test Methods for Liquid Limit, Plastic Limit, and Plasticity Index of Soils: Atterberg limits determination for soil plasticity characteristics
- ASTM D4541 - Standard Test Method for Pull-Off Strength of Coatings Using Portable Adhesion Testers: Pull-off adhesion testing with acceptance criteria >5 MPa
- ASTM D4940 - Standard Test Method for Conductimetric Analysis of Water-Soluble Ionic Contamination of Blasting Abrasives: Sandblasting procedures using angular steel grit
- ASTM D4972 - Standard Test Methods for pH of Soils: Soil pH measurements for chemical characterization
- ASTM D4973 - Standard Test Method for Sulfate in Soils: Soil electrical conductivity measurements
- ASTM D512 - Standard Test Methods for Chloride Ion In Water: Argentometric titration for chloride ion concentration verification
- ASTM D5974 - Standard Test Methods for Extractives in Adhesives: Guidelines for controlled bark incision techniques for exudate collection
- ASTM D632 - Standard Specification for Sodium Chloride: Reagent grade sodium chloride specifications (99.5% purity) for test medium preparation
- ASTM D698 - Standard Test Methods for Laboratory Compaction Characteristics of Soil Using Standard Effort: Soil compaction testing to determine optimal moisture content and maximum dry density
- ASTM D888 - Standard Test Methods for Dissolved Oxygen in Water: Dissolved oxygen content measurement in test medium (6.1 ± 0.2 mg/L)
- ASTM E1131 - Standard Test Method for Compositional Analysis by Thermogravimetry: FTIR analysis for functional group identification in exudates
- ASTM E18 - Standard Test Methods for Rockwell Hardness of Metallic Materials: Rockwell B

hardness testing using 1/16-inch steel ball indenters with 100 kgf load
- ASTM E70 - Standard Test Method for pH of Aqueous Solutions with the Glass Electrode: pH measurements of exudates using calibrated pH meters
- ASTM E8/E8M - Standard Test Methods for Tension Testing of Metallic Materials: Tensile testing using round specimens (12.5 mm diameter, 50 mm gauge length) at 0.005 s^{-1} strain rate
- ASTM G1 - Standard Practice for Preparing, Cleaning, and Evaluating Corrosion Test Specimens: Gravimetric analysis procedures and specimen cleaning protocols
- ASTM G85 - Standard Practice for Modified Salt Spray (Fog) Testing: Cyclic corrosion testing with modified protocols (4-hour cycles, 30 total cycles)
- Chaker, V. (1989). Effects of soil characteristics on corrosion. West Conshohocken, PA, USA: ASTM International.
- Chigondo, M.; Chigondo, F. (2016). Recent Natural Corrosion Inhibitors for Mild Steel: An Overview. Journal of Chemistry. Retrieved from: http://dx.doi.org/10.1155/2016/6208937.
- Dang, D.N.; Lanarde, L.; Jeannin, M.; Sabot, R.; Refait, P. (2015). Influence of soil moisture on the residual corrosion rates of buried carbon steel structures under cathodic protection. Electrochimica Acta, 176, 1410–1419.
- Dawood, M.A., Alasady, Z.M.K., Abdulazeez, M.S., Ahmed, D.S., Sulaiman, G.M., Kadhum, A.A.H., & Shaker, L.M. (2021). The corrosion inhibition effect of a pyridine derivative for low carbon steel in 1 M HCl medium: Complemented with antibacterial studies. *Int. J. Corros. Scale Inhib.*, 10(1766-1782). https://doi.org/10.17675/2305-6894-2021-10-4-1766-1782
- Dawood, M.A., Alasady, Z.M.K., Abdulazeez, M.S., Ahmed, D.S., Sulaiman, G.M., Kadhum, A.A.H., & Shaker, L.M. (2021). The corrosion inhibition effect of a pyridine derivative for low carbon steel in 1 M HCl medium: Complemented with antibacterial studies. *Int. J. Corros. Scale Inhib.*, 10, 1766–1782. https://doi.org/10.17675/2305-6894-2021-10-4-1766-1782
- Fouda, A.S., Emam, A., Refat, R., & Nageeb, M. (2017). Cascabela Thevetia Plant Extract as Corrosion Inhibitor for Carbon Steel in Polluted Sodium Chloride Solution. *Journal of Analytical & Pharmaceutical Research*, 6(1), 168-177. https://doi.org/10.15406/japlr.2017.06.00184
- Fouda, A.S.; Emam, A.; Refat, R.; Nageeb, M. (2017). Cascabela Thevetia Plant Extract as Corrosion Inhibitor for Carbon Steel in Polluted Sodium Chloride Solution. Journal of Analytical & Pharmaceutical Research, 6(1), 168-177.
- ISO 12944 - Paints and varnishes — Corrosion protection of steel structures by protective paint systems: Protective paint system standards and specifications
- ISO 4287 - Geometrical Product Specifications (GPS) — Surface texture: Profile method — Terms, definitions and surface texture parameters: Surface roughness measurement specifications and profilometer compliance (Ra = 1.6-3.2 μm)
- ISO 8501-1 - Preparation of steel substrates before application of paints and related products — Visual assessment of surface cleanliness — Part 1: Rust grades and preparation grades for uncoated steel substrates and steel substrates after overall removal of previous coatings: Surface preparation standards for Sa 2.5 cleanliness grade
- ISO 8503-1 - Preparation of steel substrates before application of paints and related products — Surface roughness characteristics of blast-cleaned steel substrates — Part 1: Specifications and definitions for ISO surface profile comparators for the assessment of abrasive blast-cleaned surfaces: Surface profile specifications (50-75 μm) after sandblasting
- Kiefner, J.F.; Rosenfeld, M.J. (2012). The Role of pipeline age in pipeline safety. INGAA Foundation, Kiefner & Associates, INC.
- Koch, G. (2017). Cost of corrosion. In *Trends in Oil and Gas Corrosion Research and Technologies* (pp. 3–30). Woodhead Publishing. https://doi.org/10.1016/B978-0-08-100777-3.00001-2
- Koch, G.; et al. (2016). International Measures of Prevention, Application, and Economics of Corrosion Technologies Study (IMPACT). NACE International: Huston, TX, USA.
- Krivy, V.; Kubzova, M.; Kreislova, K.; Urban, V. (2017). Characterization of corrosion products on weathering steel bridges influenced by chloride deposition. Metals, 7, 336.
- Li, D.G.; Bai, Z.Q.; Zhu, J.W.; Zheng, M.S. (2007). Influence of temperature, chloride ions and chromium element on the electronic property of passive film formed on carbon steel in bicarbonate/carbonate buffer solution. Electrochimica Acta, 52, 7877–7884.
- Mahmoodian, D.M. (2018). Reliability and Maintainability of In-Service Pipelines. Gulf Professional Publishing.
- Marzorati, S.; Verotta, L.; Trasatti, S.P. (2018). Green Corrosion Inhibitors from Natural Sources and Biomass Wastes. Molecules, 24, 48-73.
- NACE International. (2016). International Measures of Prevention, Application, and Economics of Corrosion Technologies Study (IMPACT). NACE International: Huston, TX, USA.
- Nnoka, M., Alaso Jack, T., & Szpunar, J. (2024). Effects of different microstructural parameters on the corrosion and cracking resistance of pipeline

steels: A review. *Eng. Fail. Anal.*, 159, 108065. https://doi.org/10.1016/j.engfailanal.2024.108065

- Okewale, A.O.; Olaitan, A. (2017). The Use of Rubber leaf Extract as a Corrosion Inhibitor for Mild Steel in Acidic Solution. International Journal of Materials and Chemistry, 7(1), 5-13.
- Owate, I.O.; Nwadiuko, O.C.; Dike, I.I.; Isu, J.O.; Nnanna, L.A. (2014). Inhibition of Mild Steel Corrosion by Aspilia africana in Acidic Solution. American Journal of Material Science, 4(3), 144–149.
- Papavinasam, S. (1999). Corrosion Inhibitors, Uhlig's Corrosion Handbook (Second Edition). Canada: John Wiley & Sons, Inc.
- Parker, M.E.; Peattie, E.G. (1984). Pipe line corrosion and cathodic protection: A practical manual for corrosion engineers, technicians, and field personnel. Houston, TX, USA: Gulf Professional Publishing.
- Pereira, R.F.C.; Oliveira, E.S.D.; Lima, M.A.G.A.; Cezar Brazil, S.L.D. (2015). Corrosion of galvanized steel under different soil moisture contents. Mater. Res., 18, 563–568.
- Putra, R.; Muhammad, A.; Huzni, S.; Fonna, S. (2020). Expecting of corrosion rate in a material affected by differences soil type in controlled environments. Materials & Corrosion Engineering Management, 1(2), 31-34.
- Singh, A.; Lin, Y.; Ebenso, E.; Liu, W.; Pan, J.; Huang, B. (2015). Gingko biloba fruit extract as an eco-friendly corrosion inhibitor for J55 steel in CO2 saturated 3.5% NaCl solution. Journal of Industrial and Engineering Chemistry, 24, 219-228.
- Sunday-Piaro, T. (2019). Performance of mild steel coated with African pear (Dacryodes edulis) resin in mud water. American Journal of Engineering Research, 8(2), 173-177.
- Usman, N.A., Tukur, U.M., & Usman, B. (2019). Comparative study on the corrosion behavior of mild steel in effluent, sea and fresh water. *Bayero Journal of Pure and Applied Sciences*, 12(1), 280–284. https://doi.org/10.4314/bajopas.v12i1.44
- Usman, N.A.; Tukur, U.M.; Usman, B. (2019). Comparative study on the corrosion behavior of mild steel in effluent, sea and fresh water. Bayero Journal of Pure and Applied Sciences, 12(1), 280 – 284.
- Verma, C., Quraishi, M., & Rhee, K.Y. (2021). Electronic Effect vs. Molecular Size Effect: Experimental and Computational based Designing of Potential Corrosion Inhibitors. *Chem. Eng. J.*, 430, 132645. https://doi.org/10.1016/j.cej.2021.132645
- Verma, C., Quraishi, M., & Rhee, K.Y. (2021). Electronic Effect vs. Molecular Size Effect: Experimental and Computational based Designing of Potential Corrosion Inhibitors. *Chem. Eng. J.*, 430, 132645. https://doi.org/10.1016/j.cej.2021.132645
- Verma, C.; Ebensoa, E.E.; Bahadura, I.; Quraishi, M.A. (2018). An Overview on Plant Extracts as Environmental Sustainable and Green Corrosion Inhibitors for Metals and Alloys in Aggressive Corrosive Media. Journal of Molecular Liquids. Retrieved from: https://doi.org/10.1016/j.molliq.2018.06.110.
- Wiese, J.D. (2015). Corrective action order, U.S. Department of Transportation Pipeline and Hazardous Materials Safety Administration Office of Pipeline Safety, Washington D.C, 20590.
- Yahaya, N.; Lim, K.S.; Norhazilan, M.N.; Othma, S.R.; Abdullah, A. (2011). Effects of clay and moisture content on soil-corrosion dynamic. Malaysian Journal of Civil Engineering, 23(1), 24-32.
- Yang, Z., Li, L., Qiao, Y., Li, C., Zhang, L., Cui, J., Ren, D., Ji, H., & Zheng, Y. (2024). Cavitation erosion-corrosion properties of as-cast TC4 and LPBF TC4 in 0.6 mol/L NaCl solution: A comparison investigation. *Ultrason. Sonochem.*, 108, 106947. https://doi.org/10.1016/j.ultsonch.2024.106947